Efficient Gene Transfer Into the Mouse Lung by Fetal Intratracheal Injection of rAAV2/6.2

Marianne Carlon[1], Jaan Toelen[1,2], Anke Van der Perren[3], Luk H Vandenberghe[4], Veerle Reumers[3], Lourenço Sbragia[2], Rik Gijsbers[1], Veerle Baekelandt[3], Uwe Himmelreich[5], James M Wilson[4], Jan Deprest[2] and Zeger Debyser[1]

[1]Molecular Virology and Gene Therapy, Department of Molecular and Cellular Medicine, Katholieke Universiteit Leuven, Flanders, Belgium; [2]Department of Woman and Child, Katholieke Universiteit Leuven, Flanders, Belgium; [3]Neurobiology and Gene Therapy, Department of Molecular and Cellular Medicine, Katholieke Universiteit Leuven, Flanders, Belgium; [4]Gene Therapy Program, Department of Pathology and Laboratory Medicine, School of Medicine, University of Pennsylvania, Philadelphia, Pennsylvania, USA; [5]Biomedical NMR Unit/Molecular Small Animal Imaging Center, Department of Medical Diagnostic Sciences, Katholieke Universiteit Leuven, Flanders, Belgium

Fetal gene therapy is one of the possible new therapeutic strategies for congenital or perinatal diseases with high mortality or morbidity. We developed a novel delivery strategy to inject directly into the fetal mouse trachea. Intratracheal (i.t.) injection at embryonic day 18 (E18) was more efficient in targeting the fetal lung than conventional intra-amniotic (i.a.) delivery. Viral vectors derived from adeno-associated virus serotype 6.2, with tropism for the airway epithelium and not earlier tested in the fetal mouse lung, were injected into the fetal trachea. Bioluminescence (BL) imaging (BLI) was combined with magnetic resonance (MR) imaging (MRI) for noninvasive and accurate localization of transgene expression *in vivo*. Histological analysis for β-galactosidase (β-gal) revealed 17.5% of epithelial cells transduced in the conducting airways and 1.5% in the alveolar cells. Stable gene expression was observed up to 1 month after injection. This study demonstrates that direct injection of rAAV2/6.2 in the fetal mouse trachea is superior to i.a. delivery for transducing the lung. Second, as stable gene transfer was detected up to 1 postnatal month, this approach may be useful to evaluate fetal gene therapy for pulmonary diseases such as cystic fibrosis, requiring both substantial numbers of transduced cells as well as prolonged gene expression to obtain a stable phenotypic effect.

Received 8 February 2010; accepted 21 June 2010; published online 27 July 2010. doi:10.1038/mt.2010.153

INTRODUCTION

Recent advances in the field of molecular and genetic diagnostics as well as high-resolution ultrasound have improved first trimester assessment of congenital or acquired conditions.[1] One of the more recent strategies is to use fetal gene transfer to treat selected congenital or perinatal diseases that have a high mortality or morbidity if left untreated, or that lead to permanent organ damage. Depending on the nature of the disease involved, fetal gene transfer should ensure permanent or transient expression of a therapeutic gene.

The rationale for prenatal gene therapy is based on several theoretic assumptions. Treatment in the prenatal period may avoid the development of early-onset disease. There is the potential of targeted delivery and prolonged exposure of proportionally smaller organs or tissues with expanding stem cell and progenitor populations. Another advantage of targeting fetal tissues is a higher vector-to-target-cell ratio that also allows viral vectors with lower titers to be used. Finally, immune tolerance associated with prenatal exposure to foreign proteins could avoid postnatal immune reactions against vector or transgenic proteins (reviewed in ref. 2).

Several viral vector systems that allow gene transfer to the fetal rodent lung have been described. Adenoviral vectors are often used because very high titers can be obtained resulting in high transduction levels of the fetal airway epithelium,[3,4] although their immunogenicity hampers long-term gene expression. Integrating lentiviral vectors can confer stable gene expression as was reported after intravascular administration of a VSV-G pseudotyped equine infectious anemia viral vector into fetal mice at embryonic day 15 (E15). This resulted in β-galactosidase (β-gal) expression in lung interstitial cells up to 79 days after injection.[5] Vector titers of lentiviral vectors, however, are often limiting resulting in limited pulmonary transduction.[6]

In recent years, recombinant adeno-associated virus (rAAV)–based vectors have been shown to efficiently transduce the adult murine airway epithelium *in vivo*.[7–10] rAAV2/2 is the best characterized and extensively studied AAV serotype, but has a limited tropism for the lung.[7] Due to isolation of novel AAV serotypes from human and nonhuman primates[11–13] and the development of transcapsidation techniques where the ITR of one serotype (mostly AAV2) can be cross-packaged into different serotype capsids (*e.g.*, AAV6.2), hybrid rAAV (*e.g.*, rAAV2/6.2) have been designed with differential tropism for specific organs (reviewed in ref. 14). rAAV2/5, rAAV2/9, and in particular rAAV2/6.2 are very efficient in transducing airway epithelium in adult mice, suggesting their use as candidate vectors for pulmonary gene therapy.[7] Furthermore, rAAVs have been shown to achieve long-term gene expression in the adult mouse lung. After intratracheal (i.t.)

The first two authors contributed equally to this work.

Correspondence: *Zeger Debyser, Kapucijnenvoer 33-VCTB+5-B7001 B-3000 Leuven, Flanders, Belgium. E-mail: Zeger.debyser@med.kuleuven.be*

instillation of a single dose of rAAV2/9 in adult mice, prolonged transgene expression was demonstrated up to 9 months after injection.[8] The superior performance of rAAV to other viral vectors may be ascribed to the capacity of rAAV to evade the host immune surveillance, although other parameters such as serotype, transgene product, route of administration, dose, and host species may play a role as well.[15] Several AAV serotypes have already been used to target the fetal rodent lung. Intra-amniotic (i.a.) administration of rAAV2/2 encoding enhanced green fluorescent protein (eGFP) at E15–E16 of gestation demonstrated gene expression in murine lungs 72 hours after injection.[16] After i.a. injection of rAAV in E24–E25 pregnant rabbits (term E31), 0.2% firefly luciferase (fLuc) positive pulmonary cells were detected 10 days after fetal vector administration.[17] In newborn rats, rAAV2/5 gave rise to moderate β-gal expression after i.t. instillation, which remained far less than what can be obtained with adenoviral vectors.[18] rAAV2/6.2 is a novel serotype that was recently shown to be more efficient for airway epithelium transduction in adult mice than other AAV serotypes.[7] To date, rAAV2/6.2 has not been tested for transduction of fetal airways.

Not only is the choice of the viral vector important, the route of administration will equally determine the efficacy of gene transfer to the targeted organ. Different access routes have been described to target the fetal rodent lung, including i.a. injection,[19–21] (ultrasound-guided) intrapulmonary injection in fetal rats[6,22] and intravenous administration into the yolk sac vessels[4,5] or umbilical vein[23] of fetal mice. We hypothesized that injection directly into the fetal mouse trachea would target the lung more specifically than systemic delivery and with higher efficiency than i.a. or intrapulmonary injection.

Therefore, we developed a new surgical procedure to target the fetal mouse lung by direct i.t. injection at the canalicular stage of lung development, which is characterized by an increase in vascularization and differentiation of epithelial precursor cells.[24] We compared delivery of fluorescent microspheres into the lung by i.t. and i.a. injection. After validating the surgical technique, we assessed the efficacy of pulmonary gene transfer by rAAV2/6.2 in this fetal mouse model. Our results demonstrate that with rAAV2/6.2, efficient transduction of fetal mouse lung can be obtained by i.t. injection. Reporter gene expression was demonstrated in 17.5% of conducting airway cells and 1.5% of alveolar cells 1 week after injection with no significant decline over a period of 4 weeks.

RESULTS

Comparison of the efficacy of intrapulmonary delivery of fluorescent microspheres by i.t. versus i.a. injection

First, we compared the efficacy of targeting the fetal mouse lung by i.t. or i.a. injection. Red 100 nm fluorescent microspheres were delivered into the fetal mouse lung by i.t. or i.a. injection in E18 pregnant Naval Medical Research Institute (NMRI) mice ($n = 5$ per group). This outbred mouse strain was chosen because of its high reproduction rate, large litter size, good maternal characteristics, and white fur, which is favorable for bioluminescence (BL) imaging (BLI). Twenty-four hours after injection, mice were killed and the corresponding fetuses harvested to examine the distribution of fluorescent microspheres in 8 µm cryosections using fluorescence microscopy. No deaths were observed at the time of harvesting. Whole-body coronal images demonstrate red fluorescent microspheres primarily in the lung as well as in the oral and nasal cavity of the i.t.-injected fetuses (**Figure 1a,c**) as opposed to the i.a.-injected ones (**Figure 1b,e**). The gastrointestinal tract was positive for both the i.t. and the i.a. group (**Figure 1d,f**). No red fluorescence was observed in other tissues from treated fetuses or in the negative control animals (data not shown).

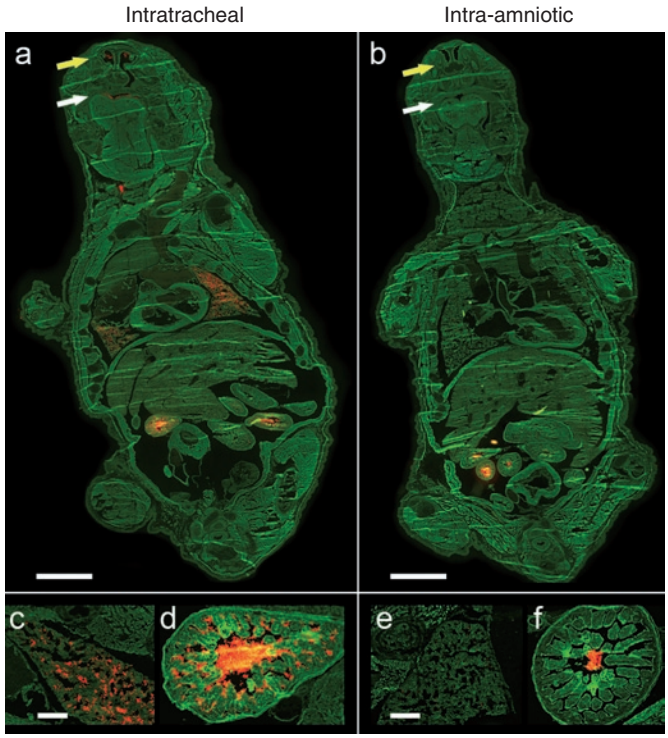

Figure 1 Comparison of the efficiency of intrapulmonary delivery of fluorescent microspheres by intratracheal (i.t.) versus intra-amniotic (i.a.) injection. (**a**,**b**) Examination of whole-body distribution of fluorescent microspheres 24 hours after i.t. or i.a. injection. **c**,**e** show the presence of fluorescent microspheres in the fetal lung after i.t. and i.a. injection, respectively. Fluorescent microspheres are also present in the oral (white arrow) and nasal (yellow arrow) cavity of the i.t.-injected fetus (**a**) and in a lower amount in the i.a.-injected fetus (**b**). (**d**,**f**) The gastrointestinal tract is positive for both the i.t.- and the i.a.-injected animal. **a**,**b**, Bar = 2 mm; **c**–**f**, bar = 200 µm.

BLI of luciferase expression following rAAV2/6.2-mediated gene delivery in the fetal lung

rAAV2/6.2 vectors encoding β-gal [2×10^9 genome copies (GC)/fetus] or fLuc (2×10^8 GC/fetus) under the control of the chicken β-actin (CBA) promoter were co-injected i.t. ($n = 8$) or i.a. ($n = 7$) in fetal NMRI mice at E18. After cesarian section and fostering, surviving pups were followed up by noninvasive BLI and monitored for fLuc activity [photons/second (p/s)] at 1 and 4 weeks of age (**Figure 2a–c**). At the first time point, the detected signal in the i.t. group [photon flux: $(1.59 \pm 1.39) \times 10^7$ p/s] was significantly higher than in the i.a. group [$(4.00 \pm 2.39) \times 10^5$ p/s, $P < 0.001$] and the uninjected control mice [$(6.03 \pm 3.61) \times 10^4$ p/s, $P < 0.01$) (**Figure 2a,c**). At 4 weeks, however, the BLI signal decreased to

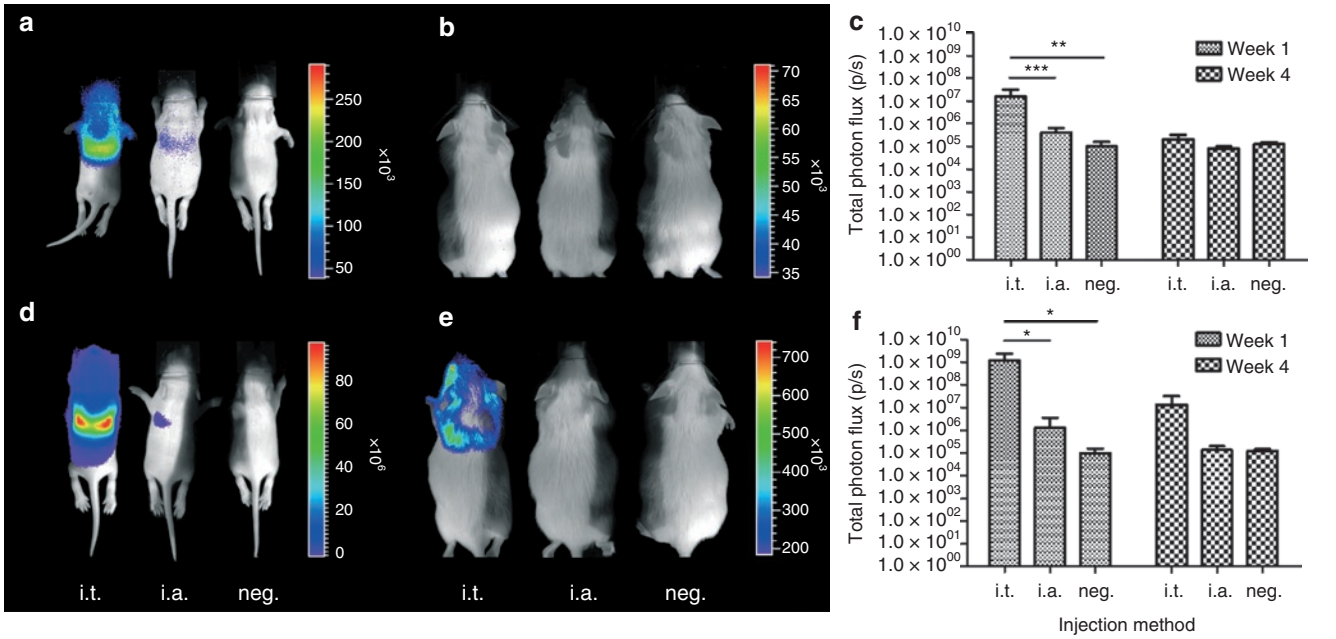

Figure 2 Bioluminescence imaging (BLI) of transgene expression after rAAV2/6.2-mediated gene delivery in fetal lung. (**a**,**b**) Low-dose rAAV2/6.2 vectors encoding β-gal [2 × 10^9 genome copies (GC)/fetus] or fLuc (2 × 10^8 GC/fetus) were co-injected i.t. or i.a. in fetal Naval Medical Research Institute mice at E18 and followed up by noninvasive BLI at 1 and 4 weeks after injection. (**c**) Quantification of total photon flux after low-dose rAAV2/6.2. (**d**,**e**) BLI signal at 1 and 4 weeks after injection after high-titer rAAV2/6.2 (3 × 10^{10} GC/fetus for β-gal and fLuc) administration with corresponding quantification of (**f**) total photon flux. All animals were scanned, separated by black partitions, to avoid scattering of photons to neighboring animals. The pseudocolor scale depicts the photon flux per second, per square centimeter per steradian (p/s/cm²/sr). Measurements were obtained in a 4.3 cm² rectangular region of interest. Please note that the scales of the BL images are different between the time points. Mean ± SD, analysis of variance, Student's *t*-test, **P* < 0.05, ***P* < 0.01, ****P* < 0.001. neg., negative.

background levels without significant difference in photon flux compared to the negative controls [(1.26 ± 0.22) ×10^5 p/s, $P = 0.2$) (**Figure 2b,c**).

The experiment was repeated with rAAV2/6.2 at higher titers (3 × 10^{10} GC/fetus for both β-gal and fLuc) with eight animals injected i.t. and six i.a. (**Figure 2d–f**). The total photon flux at week 1 for the i.t. group [(1.22 ± 0.28) ×10^9 p/s] was significantly higher than that in the i.a. group [(1.32 ± 2.34) ×10^6 p/s, $P < 0.05$] and the negative control [(6.03 ± 3.61) ×10^4 p/s, $P < 0.05$] (**Figure 2d,f**). The average BLI signal in the i.a. group [(1.32 ± 2.34) ×10^6 p/s] was not significantly higher than that in the negative control group [(6.03 ± 3.61) ×10^4 p/s, $P = 0.99$), but the variability measured in the i.a.-injected animals was high. At 4 weeks after injection, the luciferase activity in the i.t. group remained detectable [(7.31 ± 6.50) ×10^6 p/s] without reaching significance compared to the negative controls [(1.26 ± 0.22) ×10^5 p/s, $P = 0.14$] (**Figure 2e,f**).

The decrease in BLI signal at 4 weeks could relate to the limitations of the BLI technology. *In vitro* studies suggest that the reduction of BLI signal is approximately a tenfold for every centimeter of tissue depth, varying with the exact tissue type.[25] To further address this *in vivo* decrease over time, *ex vivo* luciferase enzyme activity measurements were performed on lung homogenates of the above-mentioned animals injected with high-titer rAAV2/6.2 (**Supplementary Materials and Methods, Supplementary Figure S1**). In the luciferase assay, a minor decrease in luciferase signal (~0.5 log) was observed in the i.t. group, which was, however, much less pronounced than the decrease observed with *in vivo* BLI (~2 log). Furthermore, the relative light units in this *ex vivo* assay were normalized to the total protein content of the lung extract (assessed by bicinchoninic acid assay). This might not be the ideal normalization as the protein content between a 1-and 4-week-old mouse lung can be different. Indeed, when we analyzed total protein content of negative lungs at 1 and 4 weeks of specimens with identical wet-lung weight, the 4-week-old lungs had a higher protein level (data not shown). Additionally, the small sample size and large variation prevent us to draw a statistical conclusion.

In order to assess a possible immune response, sera of mice injected with high-titer rAAV2/6.2 were collected 4 weeks after injection and analyzed for the presence of antibodies against the different transgenes (**Supplementary Materials and Methods, Supplementary Table S1**). In three out of five mice, serum antibodies were detectable. However, no correlation was seen between the presence of serum antibodies and a decrease in expression levels of the transgenes.

Combined imaging modalities for *in vivo* localization of gene expression

Since the BLI signal, when merged with a standard photographic image of the animal, only provides two-dimensional surface information of the location of gene expression, combined BL and magnetic resonance (MR) images of i.t.-injected animals were acquired at the first time point (**Figure 3**). BLI revealed a signal emanating from the neck and the thoracic region (**Figure 3a,b**). Co-registration of MRI with BLI located luciferase gene expression in the pulmonary region following a correct injection (**Figure 3e**), but in the neck and abdominal area after an incorrect

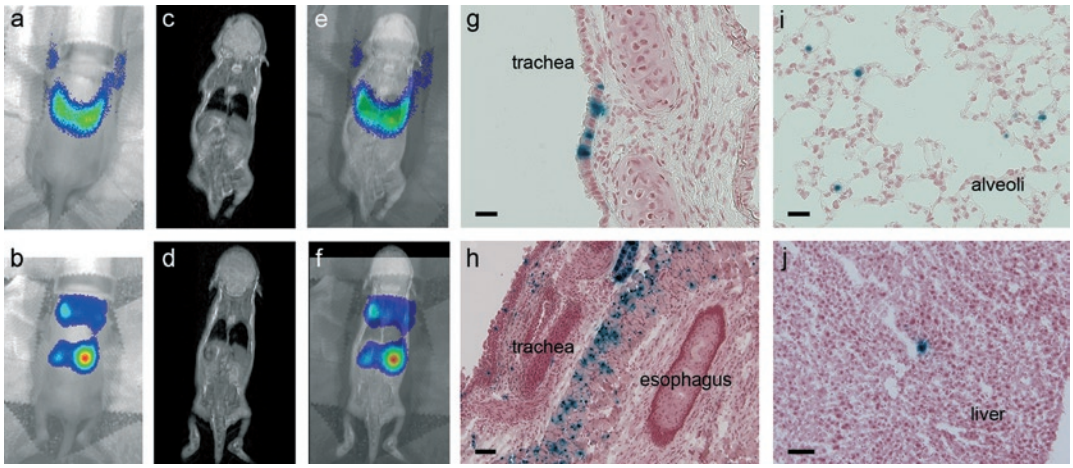

Figure 3 Combination of bioluminescence imaging (BLI) and magnetic resonance imaging (MRI) for accurate localization of gene expression *in vivo*. Combined BL-MR images of i.t.-injected animals were acquired at week 1. (**a**,**b**) BL imaging revealed a signal emanating from the neck and the upper thoracic region. (**c**,**d**) Co-registration of MRI with BLI showed that luciferase gene expression was localized in the pulmonary region after a (**e**) correct injection but in neck and abdominal area after an (**f**) incorrect injection. X-gal staining confirmed that gene expression was situated in the (**g**) conducting airways and (**i**) alveoli of the murine lung after a correct i.t. injection and in the (**h**) paratracheal space and (**j**) liver parenchyma after an incorrect i.t. injection. **g**,**i**, Bar = 25 µm; **h**,**j**, bar = 100 µm.

injection (Figure 3f). Histological analysis confirmed the *in vivo* co-registration (Figure 3).

Of note, when comparing the final survival rates of i.t.- and i.a.-injected animals, which correlates successfully fostered pups with the initial number of pups injected, survival rates were 44.7 and 56.8%, respectively (Table 1). In this respect, the i.t. injection did not result in an unacceptable loss of pups when compared to the commonly used i.a. route.

Efficiency of rAAV2/6.2-mediated gene transfer in airway epithelium of fetal mice

Final confirmation of gene expression in pulmonary epithelium was obtained by X-gal staining to visualize transduced cells. After *in vivo* imaging, animals were killed at 1 or 4 weeks after injection and lung sections stained for β-gal. After low-dose rAAV2/6.2 (2×10^9 GC/fetus β-gal; 2×10^8 GC/fetus fLuc), fetal i.t. injection resulted in 4.26 ± 0.57% transduction of the large conducting airways (trachea and mainstem bronchi) at 1 week after injection and 0.38 ± 0.17% of the alveolar cells (**Supplementary Figure S2a,b** and Figure 4a). There was no significant decline at 4 weeks in either area ($P = 0.58$ and $P = 0.7$) (**Supplementary Figure S2c,d** and Figure 4a). Histological analysis of i.a.-injected animals revealed no β-gal positive cells (data not shown).

Increased rAAV2/6.2 vector titers (3×10^{10} GC/fetus for both β-gal and fLuc) resulted in an approximately fourfold increase of transduction in the large conducting airways with 17.59 ± 1.04% β-gal positive cells and a 3.9-fold increase in the alveolar cells with 1.48 ± 0.76% transduction in the i.t.-injected group at week 1 (Figure 4b). Again, no significant decrease in transduction was detected 4 weeks after injection in either area of the lung ($P = 0.28$ and $P = 0.9$, respectively) (Figure 4b). In only one of six i.a.-injected mice, 2.04% β-gal positive cells were detected in the conducting airways at 4 weeks after injection (data not shown). Next, we analyzed the transduction efficiency of i.t. injection at different histological levels of the conducting airways (Figure 4c). At 1 week after injection, 17.87 ± 3.13% of epithelial cells were β-gal positive in the trachea, 13.13 ± 4.42% in the bronchi, and 16.16 ± 4.43% in the bronchioles (Figure 5). Four weeks after injection, no significant decrease was noted for the different regions ($P = 0.88$, $P = 0.49$, and $P = 0.1$, respectively) (Figure 5).

Table 1 Survival after intratracheal and intra-amniotic delivery of rAAV2/6.2

Injection method	Early neonatal survival rate[a]	Survival rate of fostering[b]	Final survival rate[c,d]
i.t.	38/47 (80.9%)	58.2%	21/47 (44.7%)
i.a.	32/37 (86.5%)	63.6%	21/37 (56.8%)

Abbreviations: i.a., intra-amniotic injection; i.t., intratracheal injection.
[a]Early neonatal survival, *i.e.*, after fetal surgery and at cesarean section, before fostering. [b]Pups were only fostered if they were pink, moving, and breathing normally. [c]The final survival rate is expressed as a function of the initial number of pups injected. [d]The discrepancy observed between final survivors and the number of animals included in the final cohorts of rAAV2/6.2-injected animals is due to the selective inclusion of correct injections based on noninvasive imaging (bioluminescence imaging–magnetic resonance imaging).

DISCUSSION

At present, several genetic or acquired lung diseases, which lack effective clinical treatment, could benefit from either permanent or transient expression of a therapeutic gene. Large animal models have the advantage of mimicking human lung morphology and function more closely[26] and especially chimpanzees have a high predictive value for evaluating new AAV serotypes for clinical trials as they most closely resemble humans genetically.[27] Small animal models on the other hand have been the model of choice in the field of fetal gene therapy because of the limited ethical constraints, wide availability, well-documented embryogenesis and fetal development, short gestation, large litter size, and the availability of transgenic disease models.[28] In this context, optimizing gene transfer to the fetal mouse lung is an essential step for further research of human lung diseases.

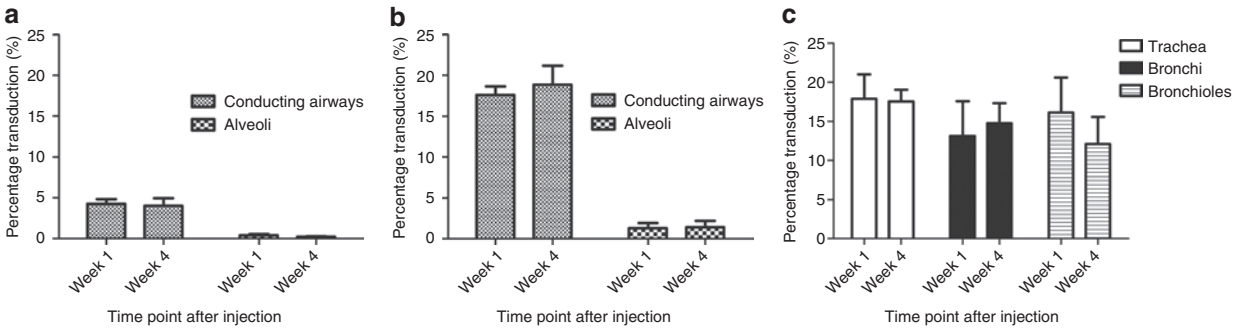

Figure 4 Transduction efficiency of rAAV2/6.2 in murine airway epithelium after fetal intratracheal injection. (**a**,**b**) Quantification of the percentage of transduced cells in conducting airways and alveoli after fetal i.t. injection of low (2×10^9 GC/fetus) and high titer (3×10^{10} GC/fetus) rAAV2/6.2, respectively. Transduction efficiency of conducting airways was determined by counting the total number of β-gal positive cells in the large airways (trachea and mainstem bronchi) relative to the total number of epithelial cells present on three cross-sections spaced 200 µm apart at ×20 magnification. Alveolar cell transduction was estimated in three cross-sections spaced 200 µm apart using a 400 × 400 µm counting frame at ×20 magnification to systematically sample the lung parenchyma of the entire lung cross-section. To determine the percentage of β-gal positive alveolar cells, the ratio of the average number of β-gal positive cells to the average cell density was made per counting frame. Transduction levels are compared between 1 and 4 weeks after vector administration. (**c**) Transduction efficiency of the conducting airways was further subdivided and quantified in the trachea, bronchi, and bronchioles, respectively, at 1 and 4 weeks after fetal i.t. injection of high-titer rAAV2/6.2. Mean ± SD, analysis of variance, Student's *t*-test, $*P < 0.05$.

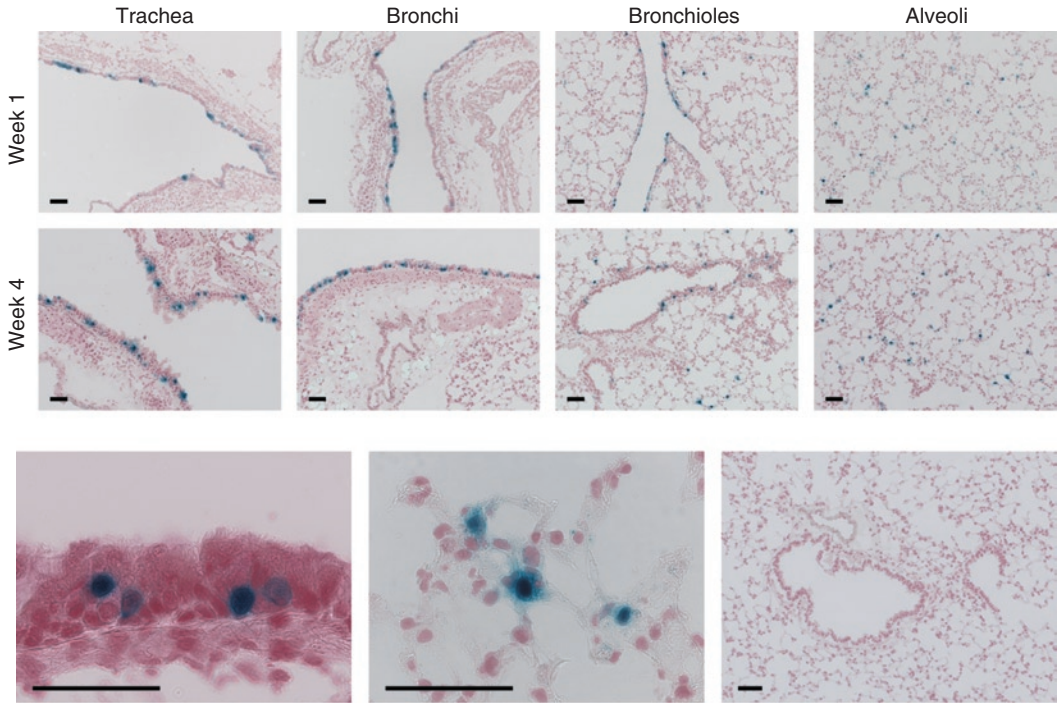

Figure 5 rAAV2/6.2-mediated transgene expression in murine airway epithelium after fetal intratracheal injection. β-gal gene transfer to the fetal mouse lung was assessed by X-gal staining. Sections were counterstained with paracarmine. Transduction efficiency is illustrated after high-dose rAAV2/6.2 vector administration (3×10^{10} GC/fetus) at weeks 1 and 4. Representative images of different lung regions are given at 1 and 4 weeks after fetal i.t. injection, respectively, showing the trachea, the bronchi, the bronchioles, and the alveoli. A high magnification image depicts β-gal positive ciliated (bottom left image) and alveolar cells (bottom middle image) at week 1. Absence of reporter gene expression in a control lung (bottom right image). Bar = 50 µm.

To date, different access routes have been described to target the fetal mouse lung, including intravenous administration into either the yolk sac vessels[5] or the umbilical vein,[23] (ultrasound-guided) intrapulmonary injection[6,22] and i.a. injection.[19–21] Systemic delivery of viral vectors is not the ideal choice for lung transduction as the vector is distributed throughout the entire body. Intrapulmonary injection, although being more specific for lung targeting, only transduces the injected area of the lung. Furthermore, ultrasound-guided intrapulmonary injection of VSV-G pseudotyped equine infectious anemia virus resulted in transduction of interstitial rather than epithelial cells, compared to i.a. delivery of the same vector.[6] These data show that different delivery routes lead to transduction of distinct cell populations.

Intra-amniotic vector delivery is the most straightforward and widely used technique to transduce fetal lungs as it is easy to perform, lacks significant mortality and is clinically acceptable.

However, marker gene expression in airway epithelium is often low and variable, with occasional transduction failure, as the viral vector is diluted by the relatively large volume of amniotic fluid. Furthermore, gene transfer depends on fetal breathing movements that, in the mouse model, are only initiated at days 15–16 (term E20–E21).[3,29] This may be enhanced by theophylline administration and exposure of the dam to elevated CO_2 levels. Yet the single most important factor proved to be the tropism and the titer of the vector preparations. Up to 97% of fetal lungs could be transduced after i.a. administration of high-titer adenoviral vectors.[3]

In larger animal models, ultrasound-guided percutaneous adenoviral vector injection into the trachea of midgestation fetal sheep has been described resulting in efficient gene transfer to the fetal trachea and bronchial tree.[30] This technique has not yet been described in a mouse model, but might be theoretically conceivable under micro-ultrasound guidance. In this model, we resorted to surgical access to the trachea. We hypothesized that direct injection into the trachea would target the lung more efficiently than i.a. delivery. We validated this microsurgical approach by fetal administration of fluorescent microspheres. Intratracheal injection was superior in targeting the fetal mouse lung compared to i.a. injection. In addition, fluorescent microspheres were also present in the nasal and oral cavity of the i.t.-injected animals. This can be explained by the reflux of particles into the fetal nose and mouth at the time of injection, as well as by fetal breathing movements, or a combination of both. Because naso- and oropharyngeal fluorescence is also seen, but to a lesser extent in the i.a.-injected group, we speculate that this is due to dilution of the fluorescent microspheres in the amniotic fluid at the time of injection. Both groups showed fluorescent microspheres in the gastrointestinal tract indicating swallowing of the fetus at E18 of gestation. These results are in line with previously published data where the uptake of fluorescent microspheres after i.a. delivery was followed up at different gestational time points ranging from E14 to E18 (ref. 20). The highest uptake in both the lungs and the gastrointestinal tract was seen at E18, the time point we used for fetal surgery.

Next, we targeted the fetal lung using rAAV2/6.2 encoding fLuc and β-gal as reporter genes. BLI is a noninvasive method for the detection and quantification of fLuc gene expression *in vivo* and thus theoretically can reduce the number of animals exposed to experimentation. This is even more valuable when a complex microsurgical protocol limits the number of treated animals and results in small cohorts for further follow-up. We observed that combining BLI and MRI at 1 week of age localized transgene expression more accurately than using BLI alone. However, sequential follow-up of transgene expression by means of BLI is challenging in a growing animal. The decrease in BLI signal observed between 1 and 4 weeks can be due to several factors: limitations of the BLI technology, loss of nonintegrated rAAV genomes after cell division, or a destructive immune response. The first reason relates to the limitations of the BLI technology. *In vitro* studies suggest that the reduction of BLI signal is approximately tenfold for every centimeter of tissue depth, varying with the exact tissue type.[25] At 1 week of age, the scanned animals are still semitransparent, lacking fur and body fat, therefore being very permissive for emitted photons. Between 1 and 4 weeks, however, they undergo major changes. Even if transgene levels would remain unchanged, the BLI signal would decrease due to increased scattering and absorption of emitted photons. Furthermore, the pharmacodynamics of the luciferin substrate might differ between a newborn and an adult mouse. In the luciferase assay, a minor decrease in luciferase signal (~0.5 log) was observed in the i.t. group, which was, however, much less pronounced than the decrease observed with *in vivo* BLI (~2 log). Furthermore, the relative light units in this *ex vivo* assay were normalized to the total protein content of the lung extract. Critics could state that this might not be the ideal normalization as the protein content between a 1- and 4-week-old mouse lung can be different. Indeed, when we analyzed total protein content of negative lungs at 1 and 4 weeks of specimens with identical wet-lung weight, the 4-week-old lungs had a higher protein level. Taken together, this shows that the decrease in BLI signal cannot be entirely explained by performing an *ex vivo* quantification of luciferase activity. The comparison between *in* and *ex vivo* luciferase signals in the lung has also been addressed by Griesenbach and co-workers[31] where they also state that *in vivo* and *ex vivo* BLI signals weakly correlate when assessed for the left lung but do not correlate when assessed for the right lung. In view of these findings, our measurement of the BLI signal *in vivo* (both left and right lung) and *ex vivo* (only left lung) have to be interpreted with caution. Additionally, the small sample size and large variation prevent us to draw a statistical conclusion.

A decrease in signal might also be due to cell division as the rAAV genome exists predominantly in an episomal state in the host nucleus, and as such depends on the turnover rate of the transduced cell types.[32] Finally, a destructive immune response against the transduced cells can account for the loss in signal.[15] We observed serum antibodies against the transgenes in three out of five mice, with no correlation between expression levels and the presence of a humoral immune response. A detailed analysis of the immune response against the rAAV capsid or the transduced cells was not a primary end point of this study. The main objective was the development of a superior delivery route for pulmonary gene transfer, which necessitated the use of the outbred NMRI strain, where the absence of genetic conformity makes a full immunological assessment challenging. Future research should ideally include an immunological assessment (in inbred mice) as destructive immune responses remain the Achilles' heel of current gene therapy trials.

β-gal was used to analyze transduction efficiency on lung cross-sections. We evaluated the percentage of β-gal positive cells in the conducting airways and alveoli separately as different genetic diseases would need a correction in either one of the two compartments. In cross-sections of adult murine lungs, transduction efficiency is routinely quantified as the number of β-gal expressing cells per high-power field.[7,8] This method is useful when analyzing lungs of adult mice, but in a growing organism, cell density changes significantly between 1 and 4 weeks of age due to lung growth and maturation.[33] Therefore, we expressed the number of β-gal positive cells relatively to the total number of cells present in the conducting airways or alveoli. In the conducting airways, we observed 17.5% transduction at 1 week after i.t. injection using high-titer rAAV2/6.2 (3×10^{10} GC/fetus β-gal). A striking observation was that the total number of β-gal expressing

cells remained stable up to 1 month after injection both in the conducting airways and alveoli. These initial results suggest that rAAV might be able to confer prolonged pulmonary gene expression following antenatal administration. Several groups have shown stable or prolonged gene expression with rAAV. Limberis and Wilson demonstrated stable β-gal expression up to 9 months in the adult mouse lung using rAAV2/9 (ref. 8). rAAV administration in the perinatal period gave rise to detectable expression in skeletal muscle and heart (at 2 months after injection),[34] as well as in lung epithelial cells (35 days after injection).[18] On the other hand, rAAV delivery targeting the neonatal rodent liver often results in transient expression levels,[35] although other groups report long-term phenotypic correction of liver disease.[36,37] The discrepancies between these observations may be explained by the different cell turnover rate of the specific organ. This is ~100 days for the tracheobronchial epithelium of adult rodents (reviewed in ref. 38). There are to our knowledge no data available on the proliferation rate prior to birth or during the first month of life. Furthermore, although rAAV is predominantly present in episomal form in the host nucleus, there is evidence that rAAV vectors can integrate into the host genome with low efficiency (reviewed in ref. 32). Clusters of transgene positive cells may indicate viral integration and subsequent clonal expansion as observed in liver tissue 4 weeks after rAAV2/8 injection in 2-day-old Gunn rats.[35] We observed clusters of β-gal expressing cells in the conducting airways at 4 weeks of life. Future experiments will have to be carried out in inbred mice to study the long-term stability of gene expression and address the immune responses against the transgene or rAAV capsids.

In conclusion, we have shown that fetal i.t. injection during the late canalicular phase of lung development with rAAV2/6.2 efficiently transduces the epithelium of the conducting airways, without a measurable decline in the number of β-gal expressing cells over a period of 4 weeks. At present, access to the fetal airways is a clinical reality[39] due to advances in fetal anesthesiology and fetoscopic instrumentation together with improvements in the field of molecular and genetic diagnostics for congenital or acquired disorders of the fetus.[1] This may open the door to fetal gene therapy for a number of perinatal diseases.

MATERIALS AND METHODS

Production of the rAAV2/6.2 vector. rAAV2/6.2 vector preparations were produced by the triple transient transfection method as previously described.[7] Briefly, for each rAAV vector preparation, 100 10-cm dishes of subconfluent, low (<50) passage HEK 293T cells (ATCC, Manassas, VA) were transfected with 30 µg plasmid DNA (pAdvDeltaF6, pRep2Cap6.2, pAAV-TF CBA-NLS-LacZ, or pAAV-TF CBA-eGFP-P2A-fLuc[40] in a ratio of 1:1:1) using a 10 µmol/l solution of 25 kDa linear polyethylenimine (in-house production). Medium was replaced the following day, and cells were harvested 2 days after transient transfection. rAAV was released from the cell lysate using three freeze–thaw cycles. The lysate was purified using an iodixanol step gradient in a Beckman Ti-70 fixed angle rotor (Analis, Ghent, Belgium) at 27,000 rpm for 2 hours. Gradient fractions were collected in 250 µl aliquots, and all fractions with a refraction index between 1.42 and 1.39 were pooled. Pooled fractions were centrifuged in a Vivaspin 6 (PES, 100 kDa cutoff; Sartorius, Göttingen, Germany) using a swinging bucket rotor at 3,000 *g*. The iodixanol of the pooled fractions was exchanged five times with phosphate-buffered saline. The final preparation was aliquoted and stored at −80 °C until further use.

Quality control of rAAV2/6.2 vector preparations

SDS–PAGE analysis: 20 µl fractions of the final vector preparations were boiled in a 6× protein loading buffer and loaded onto a 12.5% polyacrylamide gel. After electrophoresis, a silver stain procedure was performed to assess the vector purity (**Supplementary Figure S3a**). Western blotting using a monoclonal AAV antibody (anti-adeno-associated virus VP1, VP2, VP3 clone B1 mAb; American Research Products, no. 03-65158) confirmed the identity of the three bands detected by silver stain as VP1–VP3 (**Supplementary Figure S3b**).

Genomic titer: The genomic titer was determined by real-time PCR (Bio-Rad, Nazareth Eke, Belgium) according to the manufacturer's instructions. A primer probe set for the polyA sequence was used as previously described.[7] Prior to the real-time PCR, recombinant vector preparations were pretreated with DNaseI (Fermentas, St Leon-Rot, Germany). As standard, a dilution series of the rAAV transfer plasmid was used. GC obtained for the different productions ranged between 1×10^{10} and 2×10^{12} DNase-resistant GC per ml.

In utero *injection.* Time-mated pregnant outbred NMRI albino mice (Janvier, Le Genest St Isle, France) were used, the presence of a vaginal plug indicating day 1 of gestation (E1). The animals were housed under 14 hours light/10 hours dark cycle, with free access to food and water. All animal procedures were carried out under "Biosafety level 2" conditions and approved by the Biosafety Committee of the Katholieke Universiteit Leuven. Pregnant NMRI mice at E18 (term E20) were anesthetized using 1.5% isoflurane at 1 l/minute (Isoba; Intervet/Schering-Plough Animal Health, Milton Keynes, UK), and a midline laparotomy was performed to expose the uterine horns. Using a 30 G needle and a 50 µl precision syringe (Hamilton, Reno, NV), 30 µl of undiluted fluorescent microspheres (FluoSpheres; Molecular Probes, Leiden, the Netherlands) or 30 µl of viral vector suspension was injected, either through the uterine wall into the amniotic cavity or into the trachea using a stereoscopic zoom microscope (×10 magnification). Prior to i.t. injection, an incision was made in the neck region exposing the fetal trachea followed by insertion of the needle immediately distal from the larynx. Noninjected fetuses were used as negative control. Following injection, the uterine horns were repositioned within the abdomen and the abdominal wall sutured in two layers using 5/0 Vicryl absorbable sutures (Ethicon, Ascot, UK). Thereafter, the incision was infiltrated with 0.2% xylocaine (AstraZeneca, Zoetermeer, the Netherlands) for postoperative pain relief. Treated dams recovered on a heated plate and were subsequently housed individually with appropriate nesting material. At E19.5, a cesarian section was performed on the pregnant operated mice, delivering the operated fetuses, which were first marked and then placed in a foster mother's litter containing 1-day-old pups.

Tissue preparation and fluorescence microscopy. Twenty-four hours after *in utero* delivery of 30 µl red fluorescent beads via i.t. or i.a. injection, fetuses were harvested, and whole fetuses or their lungs only fixed in 10% neutral buffered formalin at 4 °C overnight. Noninjected control fetuses were processed the same way. Whole fetuses were cryopreserved in 30% sucrose (wt/vol) in phosphate-buffered saline for 3 days at 4 °C, embedded in Neg-50 (Thermo Fisher Scientific, Brussels, Belgium) and snap-frozen in liquid nitrogen–cooled isopentane. After preparation of 8 µm cryosections using a Microm HM 560 cryostat (Thermo Fisher Scientific), nuclei and actin filaments were stained with Hoechst 33258 (Sigma-Aldrich, Bornem, Belgium) and Alexa Fluor 488 phalloidin (Invitrogen, Merelbeke, Belgium), respectively, for 20 minutes at room temperature. Whole-body coronal images of injected fetuses were acquired using a Zeiss Axio-Imager equipped with a Zeiss Axiocam camera and Axiovision software (Carl Zeiss, Benelux).

Noninvasive follow-up of gene expression with BLI and MRI

BLI: Pups were followed up by BLI until the age of 1 month to determine the location and relative intensity of luciferase expression. Anesthesia was initiated in an induction chamber with 3% isoflurane in 100% oxygen at

a flow rate of 1 l/minute and maintained in the IVIS 100 system (Caliper Life Sciences, Hopkinton, MA) with a 1% isoflurane mixture at 1 l/minute. After intraperitoneal injection of D-luciferin substrate (126 mg/kg body weight dissolved in phosphate-buffered saline, 15 mg/ml; Caliper Life Sciences), a bioluminescent signal was detected in the anesthetized mice placed in ventral recumbent position. Until the maximum signal was reached, consecutive 1-minute frames were acquired. Each frame depicted the BL signal as a pseudocolor image superimposed on the gray-scale photographic image. Measurements are reported as the total photon flux from a 4.3 cm^2 rectangular region of interest.

MRI: Combined BL–micro MR (Bruker BioSpin, Ettlingen, Germany) images were acquired for all operated pups to determine the gene expression pattern. To combine BLI and MRI, a compatible animal holder was used to perform the imaging without repositioning the animals within the same anesthesia session. For co-registration of BLI and MRI, the photographic image (from BLI) was overlaid with the coronal whole-body 2D T2-weighted RARE MR image (400 µm in plane resolution, 500 µm slice thickness). Limb position and size were used to overlay BLI and MRI.

Detection of β-gal expression in lung tissue

Tissue preparation and β-gal staining: Animals were killed at two different time points (1 and 4 weeks postpartum), the right lung plus trachea embedded in Neg-50 (Thermo Fisher Scientific) and snap-frozen in liquid nitrogen–cooled isopentane. β-gal staining was performed on 6 µm frozen sections after fixation with 0.5% glutaraldehyde as previously described.[41] Mayer's paracarmine was used as a water-insoluble red counterstain to be compatible with the X-gal precipitate 5,5′-dibromo-4,4′-dichloro-indigo (Sigma-Aldrich). Sections were mounted in Mowiol and β-gal positive cells visualized using a Leica Biopoint 2 light microscope (Leica, Diegem, Belgium). Brightness and contrast were optimized using Adobe Photoshop CS3 (PC-Shop, KU Leuven, Flanders, Belgium).

Stereological quantification: Transduction efficiency of the conducting airways and alveolar cells was determined using a computerized image analysis system (StereoInvestigator; MicroBrightField, Magdeburg, Germany). Cell-type status was assigned based on the morphology of β-gal positive cells counterstained with paracarmine. Three sections, spaced ~200 µm apart, were analyzed per animal and the data presented as the number of β-gal positive cells relative to the total number of cells in the conducting airways or alveoli. To determine the percentage of positive cells in the conducting airways, the trachea, bronchi, or bronchioles were delineated, and all β-gal positive cells counted, followed by quantification of all the epithelial cells. For alveolar cell transduction, a contour was drawn around the whole lung cross-section and the section systematically sampled using the optical fractionators program. First, the cell density was estimated in each section by counting all alveolar cells in 10 counting frames (400 × 400 µm). Next, β-gal positive cells were quantified using the same size counting frame to systematically sample the lung parenchyma of the entire lung cross-section. To determine the percentage of β-gal positive alveolar cells, the ratio was made of the average number of β-gal positive cells to the average cell density per counting frame.

Statistical analysis. Data are expressed as means ± SD. Statistical significance was evaluated using the analysis of variance method to compare different treatment groups. Student's *t*-test was subsequently used for pairwise comparisons. Statistical significance was set at $P < 0.05$.

SUPPLEMENTARY MATERIAL

Figure S1. Comparison of luciferase activity after *in vivo* bioluminescence imaging and *ex vivo* enzyme activity on lung homogenates.
Figure S2. Low-titer rAAV2/6.2-mediated transgene expression in murine airway epithelium after fetal intratracheal injection.
Figure S3. Quality control of rAAV2/6.2 vector preparations.
Table S1. Evaluation of serum antibodies against transgene and comparison with transgene expression levels after fetal intratracheal injection of rAAV2/6.2.
Materials and Methods.

ACKNOWLEDGMENTS

We thank Steffi Mayer (Department of Woman and Child, Katholieke Universiteit Leuven, Flanders, Belgium) for her help in optimizing fetal surgery, Martine Michiels and Marly Balcer (Molecular Virology and Gene Therapy, Katholieke Universiteit Leuven, Flanders, Belgium), and Ann Van Santvoort (Biomedical NMR Unit/Molecular Small Animal Imaging Center, Katholieke Universiteit Leuven, Flanders, Belgium) for their excellent technical assistance. M.C., J.T., and A.V.d.P. are doctoral fellows supported by grants from the Institute for the Promotion of Innovation through Science and Technology in Flanders (IWT-Vlaanderen). Research was funded by IWT-Vlaanderen, by the EC grant DIMI (LSHB-CT-2005-512146) and the Molecular Small Animal Imaging Center (MoSAIC) from the KU Leuven. L.H.V. holds patents on technology described within. J.M.W. is an inventor on patents licensed to various biopharmaceutical companies including ReGenX for which he has equity in, consults for and receives a grant from.

REFERENCES

1. Scotet, V, Duguépéroux, I, Audrézet, MP, Blayau, M, Boisseau, P, Journel, H *et al.* (2008). Prenatal diagnosis of cystic fibrosis: the 18-year experience of Brittany (western France). *Prenat Diagn* **28**: 197–202.
2. Coutelle, C, Themis, M, Waddington, SN, Buckley, SM, Gregory, LG, Nivsarkar, MS *et al.* (2005). Gene therapy progress and prospects: fetal gene therapy–first proofs of concept–some adverse effects. *Gene Ther* **12**: 1601–1607.
3. Buckley, SM, Waddington, SN, Jezzard, S, Lawrence, L, Schneider, H, Holder, MV *et al.* (2005). Factors influencing adenovirus-mediated airway transduction in fetal mice. *Mol Ther* **12**: 484–492.
4. Waddington, SN, Nivsarkar, MS, Mistry, AR, Buckley, SM, Kemball-Cook, G, Mosley, KL *et al.* (2004). Permanent phenotypic correction of hemophilia B in immunocompetent mice by prenatal gene therapy. *Blood* **104**: 2714–2721.
5. Waddington, SN, Mitrophanous, KA, Ellard, FM, Buckley, SM, Nivsarkar, M, Lawrence, L *et al.* (2003). Long-term transgene expression by administration of a lentivirus-based vector to the fetal circulation of immuno-competent mice. *Gene Ther* **10**: 1234–1240.
6. Henriques-Coelho, T, Gonzaga, S, Endo, M, Zoltick, PW, Davey, M, Leite-Moreira, AF *et al.* (2007). Targeted gene transfer to fetal rat lung interstitium by ultrasound-guided intrapulmonary injection. *Mol Ther* **15**: 340–347.
7. Limberis, MP, Vandenberghe, LH, Zhang, L, Pickles, RJ and Wilson, JM (2009). Transduction efficiencies of novel AAV vectors in mouse airway epithelium *in vivo* and human ciliated airway epithelium *in vitro*. *Mol Ther* **17**: 294–301.
8. Limberis, MP and Wilson, JM (2006). Adeno-associated virus serotype 9 vectors transduce murine alveolar and nasal epithelia and can be readministered. *Proc Natl Acad Sci USA* **103**: 12993–12998.
9. Auricchio, A, O'Connor, E, Weiner, D, Gao, GP, Hildinger, M, Wang, L *et al.* (2002). Noninvasive gene transfer to the lung for systemic delivery of therapeutic proteins. *J Clin Invest* **110**: 499–504.
10. Halbert, CL, Allen, JM and Miller, AD (2001). Adeno-associated virus type 6 (AAV6) vectors mediate efficient transduction of airway epithelial cells in mouse lungs compared to that of AAV2 vectors. *J Virol* **75**: 6615–6624.
11. Gao, G, Vandenberghe, LH, Alvira, MR, Lu, Y, Calcedo, R, Zhou, X *et al.* (2004). Clades of Adeno-associated viruses are widely disseminated in human tissues. *J Virol* **78**: 6381–6388.
12. Gao, GP, Alvira, MR, Wang, L, Calcedo, R, Johnston, J and Wilson, JM (2002). Novel adeno-associated viruses from rhesus monkeys as vectors for human gene therapy. *Proc Natl Acad Sci USA* **99**: 11854–11859.
13. Vandenberghe, LH, Breous, E, Nam, HJ, Gao, G, Xiao, R, Sandhu, A *et al.* (2009). Naturally occurring singleton residues in AAV capsid impact vector performance and illustrate structural constraints. *Gene Ther* (epub ahead of print).
14. Choi, VW, McCarty, DM and Samulski, RJ (2005). AAV hybrid serotypes: improved vectors for gene delivery. *Curr Gene Ther* **5**: 299–310.
15. Vandenberghe, LH and Wilson, JM (2007). AAV as an immunogen. *Curr Gene Ther* **7**: 325–333.
16. Garrett, DJ, Larson, JE, Dunn, D, Marrero, L and Cohen, JC (2003). *In utero* recombinant adeno-associated virus gene transfer in mice, rats, and primates. *BMC Biotechnol* **3**: 16.
17. Boyle, MP, Enke, RA, Adams, RJ, Guggino, WB and Zeitlin, PL (2001). *In utero* AAV-mediated gene transfer to rabbit pulmonary epithelium. *Mol Ther* **4**: 115–121.
18. Fleurence, E, Riviere, C, Lacaze-Masmonteil, T, Franco-Motoya, ML, Waszak, P, Bourbon, J *et al.* (2005). Comparative efficacy of intratracheal adeno-associated virus administration to newborn rats. *Hum Gene Ther* **16**: 1298–1306.
19. Buckley, SM, Waddington, SN, Jezzard, S, Bergau, A, Themis, M, MacVinish, LJ *et al.* (2008). Intra-amniotic delivery of CFTR-expressing adenovirus does not reverse cystic fibrosis phenotype in inbred CFTR-knockout mice. *Mol Ther* **16**: 819–824.
20. Davies, LA, Varathalingam, A, Painter, H, Lawton, AE, Sumner-Jones, SG, Nunez-Alonso, GA *et al.* (2008). Adenovirus-mediated *in utero* expression of CFTR does not improve survival of CFTR knockout mice. *Mol Ther* **16**: 812–818.
21. Mitchell, M, Jerebtsova, M, Batshaw, ML, Newman, K and Ye, X (2000). Long-term gene transfer to mouse fetuses with recombinant adenovirus and adeno-associated virus (AAV) vectors. *Gene Ther* **7**: 1986–1992.

22. Toelen, J, Deroose, CM, Gijsbers, R, Reumers, V, Sbragia, LN, Vets, S *et al.* (2007). Fetal gene transfer with lentiviral vectors: long-term *in vivo* follow-up evaluation in a rat model. *Am J Obstet Gynecol* **196**: 352.e1–352.e6.
23. Senoo, M, Matsubara, Y, Fujii, K, Nagasaki, Y, Hiratsuka, M, Kure, S *et al.* (2000). Adenovirus-mediated *in utero* gene transfer in mice and guinea pigs: tissue distribution of recombinant adenovirus determined by quantitative TaqMan-polymerase chain reaction assay. *Mol Genet Metab* **69**: 269–276.
24. Kaufman, MH (1992). *The Atlas of Mouse Development*. Academic: New York. pp. 445–448.
25. Contag, CH, Contag, PR, Mullins, JI, Spilman, SD, Stevenson, DK and Benaron, DA (1995). Photonic detection of bacterial pathogens in living hosts. *Mol Microbiol* **18**: 593–603.
26. Casal, M and Haskins, M (2006). Large animal models and gene therapy. *Eur J Hum Genet* **14**: 266–272.
27. Flotte, TR, Fischer, AC, Goetzmann, J, Mueller, C, Cebotaru, L, Yan, Z *et al.* (2010). Dual reporter comparative indexing of rAAV pseudotyped vectors in chimpanzee airway. *Mol Ther* **18**: 594–600.
28. Scholte, BJ, Davidson, DJ, Wilke, M and De Jonge, HR (2004). Animal models of cystic fibrosis. *J Cyst Fibros* **3** (suppl. 2): 183–190.
29. Douar, AM, Adebakin, S, Themis, M, Pavirani, A, Cook, T and Coutelle, C (1997). Foetal gene delivery in mice by intra-amniotic administration of retroviral producer cells and adenovirus. *Gene Ther* **4**: 883–890.
30. Peebles, D, Gregory, LG, David, A, Themis, M, Waddington, SN, Knapton, HJ *et al.* (2004). Widespread and efficient marker gene expression in the airway epithelia of fetal sheep after minimally invasive tracheal application of recombinant adenovirus *in utero*. *Gene Ther* **11**: 70–78.
31. Griesenbach, U, Meng, C, Farley, R, Cheng, SH, Scheule, RK, Davies, MH *et al.* (2008). *In vivo* imaging of gene transfer to the respiratory tract. *Biomaterials* **29**: 1533–1540.
32. McCarty, DM, Young, SM Jr and Samulski, RJ (2004). Integration of adeno-associated virus (AAV) and recombinant AAV vectors. *Annu Rev Genet* **38**: 819–845.
33. Warburton, D, Gauldie, J, Bellusci, S and Shi, W (2006). Lung development and susceptibility to chronic obstructive pulmonary disease. *Proc Am Thorac Soc* **3**: 668–672.
34. Wang, Z, Zhu, T, Qiao, C, Zhou, L, Wang, B, Zhang, J *et al.* (2005). Adeno-associated virus serotype 8 efficiently delivers genes to muscle and heart. *Nat Biotechnol* **23**: 321–328.
35. Flageul, M, Aubert, D, Pichard, V, Nguyen, TH, Nowrouzi, A, Schmidt, M *et al.* (2009). Transient expression of genes delivered to newborn rat liver using recombinant adeno-associated virus 2/8 vectors. *J Gene Med* **11**: 689–696.
36. Ghosh, A, Allamarvdasht, M, Pan, CJ, Sun, MS, Mansfield, BC, Byrne, BJ *et al.* (2006). Long-term correction of murine glycogen storage disease type Ia by recombinant adeno-associated virus-1-mediated gene transfer. *Gene Ther* **13**: 321–329.
37. Kügler, S, Hahnewald, R, Garrido, M and Reiss, J (2007). Long-term rescue of a lethal inherited disease by adeno-associated virus-mediated gene transfer in a mouse model of molybdenum-cofactor deficiency. *Am J Hum Genet* **80**: 291–297.
38. Rawlins, EL and Hogan, BL (2006). Epithelial stem cells of the lung: privileged few or opportunities for many? *Development* **133**: 2455–2465.
39. Deprest, J, Gratacos, E and Nicolaides, KH; FETO Task Group (2004). Fetoscopic tracheal occlusion (FETO) for severe congenital diaphragmatic hernia: evolution of a technique and preliminary results. *Ultrasound Obstet Gynecol* **24**: 121–126.
40. Ibrahimi, A, Vande Velde, G, Reumers, V, Toelen, J, Thiry, I, Vandeputte, C *et al.* (2009). Highly efficient multicistronic lentiviral vectors with peptide 2A sequences. *Hum Gene Ther* **20**: 845–860.
41. Limberis, M, Bell, P and Wilson, JM (2007). Detection of reporter gene expression in murine airways. *Methods Mol Biol* **411**: 25–34.